Geophysical Model Development Discussion gmd-2019-272-RC3

Representation of the Denmark Strait Overflow in a z-coordinate eddying configuration of the NEMO (v3.6) ocean model: Resolution and parameter impacts" by Pedro Colombo et al.

Response to the Reviewer 3

We greatly appreciated this extensive and detailed review which raised interesting issues and helped to largely improve the clarity of our manuscript. In the following, we provide our responses in a point-by-point manner. In our responses below, we use the following legend:

- *Italic characters* for the Reviewers' comments.
- Blue color for our answers to the comments.
- *Blue color in italic* for the revised text, changes being sometimes outlined in *magenta*.

Reviewer's comment 1.
Absence of figures with observations. It is very hard to follow the text, when the authors refer to figures in the other papers. I found only one plot (Fig 16) to be very informative. Is it possible to plot similar figures from observations? I believe that most of the observed data are present in databases such as EN4.
We agree with the reviewer that referring to figures published in other papers does not make the reading easy. Following the recommendations, we added figures with observations.

Modification of Figure 4:
This figure now includes the section from Mastropole et al. (M2017) in the paper, such that our assessment of the properties of the overflow "source waters" that compares the model data with M2017 data (Section 2.3) does not require going back and forth between our figure and the figure shown in M2017. We obtained the observation data from R. Pickart group at WHOI. The Figure legend and the text have been modified as follows in the revised version of the paper.

New Figure 4:

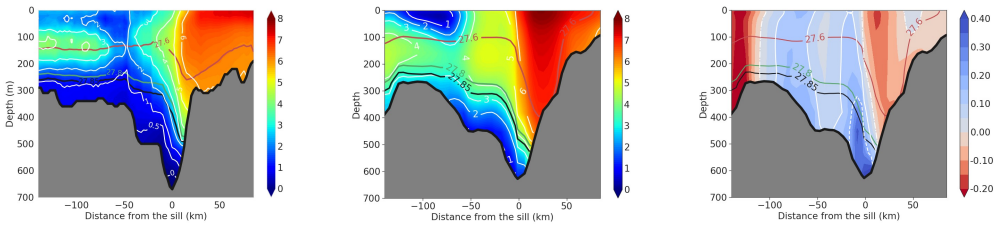

(a) Observations (b) DSO12.L46 (c) DSO12.L46

"Figure 4. Mean flow characteristics (annual mean of year 76) in the global simulation at the sill. Temperature (°C) in colours and white contours for (a) the observations (Mastropole et al., 2017) and (b) the control simulation (1/12° and 46 vertical levels). Potential density values (σ_0) are shown by the contour lines coloured in red (27:6), green (27:8) and black (27:85). (c) The velocity normal to the section in the control simulation (southward velocity in blue colour being negative). White lines indicate the 0 ms^{-1} contour (dotted line), the -0.1 ms^{-1} (full line) and the -0.2 ms^{-1} contour (dashed line). The model section being taken along the model coordinate, the topography is slightly different in the model."

The text now reads (page 8 starting line 24):
"Fig. 4 presents the characteristics of the mean flow across the sill. The model simulation is compared to the data of Mastropole et al. (2017) who processed over 110 shipboard hydrographic sections across Denmark Strait (representing over 1000 temperature and salinity profiles) to estimate the mean conditions of the flow at the sill (Fig. 4a). The model simulation (Fig. 4b) shows a similar distribution of the isopycnals, specially the location of the 27.8 isopycnal. However, the observations exhibit waters denser than 28.0 in the deepest part of the sill which the model does not reproduce. Large flaws are noticed regarding the temperature of the deepest waters which are barely below 1°C when observations clearly show temperatures below 0°C (also

seen in the observations presented in e.g. Jochumsen et al., 2012, Jochumsen et al., 2015, Zhurbas et al., 2016). A bias toward greater salinity values (not shown) is also found in the control experiment which shows bottom salinity of 34.91 compared to 34.9 in the observations shown in Mastropole et al. (2017), but the resulting stratification in density (Fig. 4b) shows patterns that are consistent with observations. The distribution of velocities (Fig. 4c) is also found realistic when compared with observations (i.e. the Fig. 2b of Jochumsen et al., 2012) with a bottom intensified flow of dense waters (up to 0.4 ms^{-1}) in the deepest part of the sill. Although the present setup is designed to investigate model sensitivity in twin experiments and not for comparison with observations ends, the control run appears to provide a flow of dense waters at the sill that is stable over the 5 year period of integration and reproduces qualitatively the major patterns of the overflow "source waters" seen in the observations. Therefore, despite existing biases, the presence of a well identified dense overflow at the sill confirms the adequacy of the configuration for the sensitivity studies."

Additional Figure (New Figure 5):
We added a new figure comparing the model with observations at the downstream-most section among those shown in the paper (i.e. section 29 in Fig. 1). We chose that section because :

- it is a good illustration of the major flaws of the "end product" in the Control run (the plume is too warm, diluted, does not reach deep enough, and is hardly distinguishale from the ambient fluid), and therefore it complements Fig 4 which shows the "source waters".
- It provides guidance regarding assessment of improvement: improvements will be akcnowledged if the plume is colder, or deeper, or separated from the ambient fluid by sharper gradients.

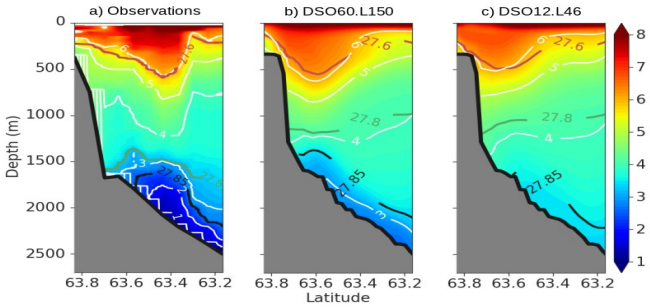

Figure 5: Potential Temperature (°C) at section 29 in (a) the observations (ASOF6-section, Quadfasel, 2004), (b) the 1/60°, 150 levels simulation, and (c) the 1/12°, 46 level simulation. Red/Green/Black full lines are isopycnals 27.6/27.8/27.85. White lines are isotherms by 1°C interval. For panel b), the section 29 is outside (~100 km downstream) the 1/60° AGRIF zoom, so the effective resolution is 1/12°. But the water masses acquired their properties upstream within the 1/60° resolution zoom. Observation data were downloaded at https://doi.pangaea.de/10.1594/PANGAEA.890362.

Modifications brought to the text (page 9, line 6 and following):
"Finally, in order to assess improvements in the sensitivity tests, the major flaws of the control simulation must be described. If similarities with observations are found at the sill, the evolution of the DSO plume in the Irminger basin is shown to be unrealistic in the present setup of the control simulation, and presents the same flaws as in the global run. This is demonstrated by the analysis of the temperature and potential density profiles at the most downstream cross-section (section 29) where the model solution is compared to observations (Fig. 5), and at the other cross-sections along the path of the DSO in the Control simulation (the plots on the left hand side of Fig. 6 and 7). The evolution of the DSO plume as it flows southward along the East Greenland shelf break is represented by a well-marked bottom boundary current (e.g. the bottom currents in Fig. 2) carrying waters of greater density than the ambient waters. Far downstream the sill (section 29) the observations show a well-defined plume of cold water confined below the 27.8 isopycnal under 1500 m depth (Fig. 5a). The bottom temperature is still below 1°C. In the Control simulation (Fig. 5c), one can clearly identify the core of the DSO plume with the 27.85 isopycnal below 1500 m, so it is clear that the plume has been sinking to greater depth as it moved southward. This evolution is only qualitatively consistent with the observations at this section because the modelled plume is significantly warmer, exhibiting a temperature of 3.5° (against 2°C or less in the observations). The temperature and salinity gradients separating the plume from the interior ocean are smaller than observed, indicating a greater dilution with ambient waters. The plume is barely distinguishable from the ambient fluid below 2000m when it is still well marked at that depth in the observations. The sinking and dilution of the plume as it flows

southward along the slope of the Greenland shelf are also well illustrated in Fig. 6 and 7 (left hand panels) which display the potential temperature at the other sections. If the overflow waters are still well-marked at section 16 (Fig. 6a), they are barely distinguishable from the ambient water at section 29."

Reviewer's comment 2.
Secondly the introduction of the manuscript is not satisfactory written, the style and organisation of paragraphs require clarifications and improvements. Please answer the following questions:
What is an overflow? How and where do overflows originate? How long do they propagate? Relative thickness, velocity, range of mass fluxes? Why it is so important in global simulations: e.g Impact on the Global Conveyer belt (MOC)? What are the main balance of forces in the overflows! Why is the fine resolution needed, what processes should be resolved in the ideal case? What is the problem in overflow simulation by z-coordinate models, show the numbers! say predicted temperature 3C higher, etc.

The information suggested by the reviewers' questions would likely be necessary in a review paper, or a study having for objective to reach the most realistic simulation of the overflows (i.e. accurately comparing with observations), as done in the studies of e.g. Magaldi et al. (2015), Koszalka et al. (2017), Almansi et al. (2017) or Spall et al. (2019). But the scope of our paper is different. The objective is to explore and document the limitations for the NEMO ocean circulation model to represent the overflow of the Denmark Strait, in a context that is relevant for global model simulations, i.e. with resolution and parameterisations now used in global model simulations. We consider that the introduction of the paper is broad enough to introduce the objective. It is already quite long (3 pages), and most questions raised by the reviewer were already addressed, but with less details than the reviewer suggested. Also, answers to some of the reviewer's questions were given in Section 2.3 when we assessed the solution of the control run and describe the major flaws of this simulation.

Nevertheless, the reviewer's comments indicate that the introduction can be improved. So we carefully went through it again and re-structured and modified several paragraphs in an attempt to account for the questions asked.

The introduction is now structured in eight paragraphs which address the following items:

- What is an overflow.
- Why overflows are important.
- Important processes and their representation in OGCMs.
- State of the art in direct simulations of overflows.
- Status of and issues relevant to global eddying models.
- Rationale of the study: what is needed to improve understanding.
- Objectives of the study.
- Outlines of the paper.

We indicate below the content of each paragraph, and we emphasize in magenta the text that directly answers the reviewer's questions.

(What is an overflow)

"Oceanic overflows are gravity currents flowing over topographic constraints like narrow straits, channels or sills, and down topographic slopes. Overflows carry dense waters formed in marginal seas or on continental shelves through intense air-sea exchanges (cooling, evaporation) from their source regions into the great ocean basins where they join the general ocean circulation (Legg et al., 2006, 2007). Overflows are often structured as plumes or boluses of dense fluid thick of a few hundred meters, accelerated toward great depths by gravity (Magaldi and Haine, 2015, Koszalka et al., 2017, Almansi et al., 2017, or Spall et al., 2019). As they cascade down over distances that may reach up to a few hundreds of kilometers with mean velocities varying between 0.25 to 1 ms^{-1}, they entrain ambient waters through advection and intense shear-driven mixing processes. After reaching a depth close to a neutral buoyancy level and a quasi-geostrophic equilibrium, the entrainment of ambient water is significantly reduced and the overflow becomes a neutrally buoyant bottom density current (Legg et al., 2009, Danabasoglu et al., 2010)."

(Why overflows are important)

"Overflows of importance because of their contribution to the general circulation are those associated with; the Denmark Strait and the Faroe Bank Channel where dense cold waters formed in the Arctic Ocean and the Nordic Seas flows into the North Atlantic (Girton and Standford, 2003, Hansen and Østerhus, 2007, Quadfasel and Käse, 2007, Brearley et al., 2012); the strait of Gibraltar where dense saline waters generated in the Mediterranean Sea overflow into the Atlantic Ocean (Baringer and Price, 1997); the strait of Bab-el-Manded where the highly saline Red Sea waters flow into the Gulf of Aden and the Indian ocean (Peters et al., 2005), and the continental shelves of the polar oceans (Killworth, 1977, Baines and Condie, 1998), in particular around Antarctica where the high salinity shelf waters formed in Polynyas ventilate the Antarctic Bottom waters (Mathiot et al., , Purkey et al., 2018). More reference papers can be found in Legg et al. (2009), Magaldi et al. (2015), Mastropole et al. (2017). Altogether, these overflows feed most of the world ocean deep waters and play an important role distributing heat and salt in the ocean. For the case of the Denmark Strait overflow (DSO hereafter), it feeds the Deep Western Boundary Current in the North Atlantic, and so contributes to the Atlantic Meridional Overturning Cell and the global thermohaline circulation (Dickson and Brown, 1994, Beismann and Barnier, 2004, Hansen and Østerhus, 2007, Dickson et al., 2008, Yashayaev and Dickson, 2008, Danabasoglu et al., 2010, Zhang et al., 2011, von Appen et al., 2014). This world-ocean wide importance of the overflows makes their representation a key aspect of ocean general circulation models (OGCMs)."

(Important processes and their representation in OGCMs)
"A variety of physical processes of different scales are involved in the control of overflows and their mixing with the ambient waters (Legg et al., 2007). Dynamical processes (e.g. hydraulic control/jump at sills/straits, mesoscale instability of the dense water plume, interactions of the plume with overlaying currents), have length scales of a few kilometers in the horizontal and a few tens of meters in the vertical. Such scales of motion are not resolved in present large-scale coarse resolution (non-eddying) ocean models used for climate studies but can be simulated in eddy-resolving models (Legg et al., 2007, 2008). Diapycnal mixing processes (e.g. entrainment of ambient waters into the cascading plume by shear-driven mixing, bottom friction, internal wave breaking) have even smaller scales (a few meters to a 1 mm) and cannot be resolved in present ocean models. Their effects are represented by a vertical turbulence closure scheme, the aim of which is to achieve a physically-based representation of this small-scale turbulence. However, models using fixed geopotential levels as vertical coordinate (i.e. z-level models) are known to generate spurious (i.e. excessive and non-physical) diapycnal mixing when moving dense overflow waters downslope. The link of this spurious mixing with the staircase-like representation of the bottom topography peculiar to these models is well established (Winton et al., 1998, Wang et al., 2008). The parameterisation of overflows in these models has been the topic of a number of studies (Beckmann and Döscher, 1997, Campin et al., 2012, Killworth and Edwards, 1999, Song and Chao, 2000, Danabasoglu et al., 2010, Wang et al., 2015). A large number of idealized model studies, many of them conducted in the DOME framework (Dynamics of Overflows Mixing and Entrainment, Legg et al., 2006, Legg et al., 2009), tested the ability of overflow parameterizations against very high-resolution simulations in a variety of OGCMs. When used in global simulations these parameterisations improve overflows, but still produce deep or bottom water properties that are not yet satisfactory if not inadequate (Condie et al., 1995, Griffies et al., 2000, Legg et al., 2009, Danabasoglu et al., 2010, Danabasoglu et al., 2014, Downes et al., 2011, Weijer, 2012, Heuzé et al., 2013, Wang et al., 2015, Snow et al., 2015). Past model studies performed with DOME-like idealized configurations also permitted to gain understanding on the dynamics of overflows and on the sensitivity of their representation in models to physical and numerical parameters (see Reckinger et al., 2015, for exhaustive references and a synthesis of the main findings). Significant differences between models due to the type of vertical coordinate system were pointed out (e.g. Ezer and Mellor, 2004, Legg et al., 2006, Wang et al., 2008, Laanaia et al., 2010, Wobus et al., 2011, Reckinger et al., 2015)."

(State of the art in direct simulations of overflows)
"Numerical modelling of dense water cascades with OGCMs designed to simulate the large scale circulation still represents a challenge, especially because the hydrostatic approximation on which these model rely remove the vertical acceleration from the momentum equation. This results in a misrepresentation of the diapycnal mixing processes (Özgökmen, 2004) and requires, to represent their effects, a turbulence closure scheme. Magaldi and Haine (2015), compared high-resolution (2 km) hydrostatic and non-hydrostatic simulations of dense water cascading in a realistic model configuration of the Irminger basin. They found that for such 2 km horizontal resolution, the parameterization of the non-resolved turbulence used in the

hydrostatic model was accurately representing the effects of the lateral stirring and vertical mixing associated with the cascading process.
Most recent high-resolution regional modelling studies of the Denmark Strait overflow (Magaldi et al., 2011, Koszalka et al., 2013, 2017, Almansi et al., 2017, Spall et al., 2019) or the Faroe Bank Chanel overflow (Riemenschneider and Legg, 2007, Seim et al., 2010) have been using hydrostatic model configurations of the MIT OGCM. These studies, as they provide modelled overflows in good agreement with observations, significantly improved the actual understanding of the overflows and their modelling. For the case of the DSO, the studies referred above especially pointed out the importance of the resolution of the cyclonic eddies linked to the dense overflow water boluses on the entrainment, and the importance of the dense water cascading from the East Greenland Shelf with the Spill Jet. On the modelling aspects, these studies provided some rationale regarding the grid-resolution that permit a representation of the overflows that agrees with observations (a resolution of 2 km in the horizontal and a few tens of meters near the bottom in the vertical). They also characterized the dependence on various model parameters regarding the mixing of the overflow waters with ambient waters. For the case of the Faroe Bank Channel overflow for example, Riemenschneider and Legg (2007) found the greatest sensitivity of the mixing in changes in horizontal resolution. However, the high resolution used in these regional studies cannot yet be used in eddying global model hindcast simulations of the last few decades or for eddying ensemble simulations."

(Status of and issues relevant to global eddying models)
"Indeed, global eddying OGCM are now commonly used at resolutions of 1/12°, which yields a grid-size of about 5 km in the region of the Nordic Seas overflows and may resolve with some accuracy the entrainment of ambient waters into the overflow plume by eddy-driven advection, but not the small-scale diapycnal mixing which still needs to be fully parameterized by the turbulence closure scheme. Chang et al. (2009) studied the influence of horizontal resolution on the relative magnitudes and pathways of the Denmark Strait and Iceland-Scotland overflows in a North Atlantic configuration of the HYCOM OGCM (Chassignet et al. (2003)). They found that at 1/12°, the highest resolution tested, the simulations show realistic overflow transports and pathways and reasonable North Atlantic three-dimensional temperature and salinity fields. The ability of HYCOM to represent the spreading of the overflow waters at 1/12° resolution was later confirmed by the studies of Xu et al. (2010), Xu et al. (2014). Marzocchi et al. (2015), provided an assessment of the ocean circulation in the subpolar North Atlantic in a 30-years long hindcast simulation performed with the ORCA12 configuration, a z-coordinate partial-step global implementation of the NEMO OGCM (Madec et al., 2016) at 1/12° resolution developed by the Drakkar Group (2014). They found that the model had some skills as the volume transport and variability of the overflows from the Nordic Seas were reasonably well represented. However, significant flaws were found in the overflow water mass properties that were too warm (by 2.5 to 3°C) and salty. This latter bias can be partly attributed to the excessive entrainment peculiar to the z-coordinate, but other sources of biases, like the warm and salty bias found in the entrained waters of the Irminger basin, a resisting bias in this type of model simulations (Treguier et al., 2005, Rattan et al., 2010), are likely to contribute."

(Rationale of the study: what is needed to improve understanding)
"Despite the progresses reported above, it is clear that overflow representation is still a resisting flaw in z-coordinate hydrostatic ocean models. NEMO (version 3.6) is now commonly used in eddying (1/4° to 1/12°) configurations for global or basin-scale, climate-oriented studies (e.g. Megan et al., 2014, Williams et al.,2015, Treguier et al., 2017, Sérazin et al., 2018), reanalyses and operational forecasts (Lellouche et al., 2013, Lellouche et al., 2018, Le Traon et al., 2017), or ensemble multi-decadal hindcast simulations (Bessières et al., 2017, Penduff et al., 2018). Even though their use by a growing community, model configurations like ORCA12 remain computationally expensive and sensitivity studies are limited. Therefore, there is a need to establish the sensitivity of the simulated overflows to the available parameterizations in a realistic framework relevant to the commonly used resolutions."

(Objectives of the study)
"The objective of this work is to provide a comprehensive assessment of the representation of overflows by NEMO in a realistic eddy-permitting to eddy-resolving configuration that is relevant for many present global simulations performed with this model, in particular with the standard 1/12° ORCA12 configuration setup similar to that presently used for operational forecasting by the CMEMS[1]. Therefore, we limit our investigation to the sensitivity of the overflow representation when standard parameters or resolution are varied, the objective being to identify the model parameters and resolutions of significant influence.

However, because NEMO is also used at much higher resolution (1/60°, e.g. Ducousso et al., 2017) and offers possibilities of local grid refinement (Debreu et al., 2007) already used with success (e.g. Chanut et al., 2008, Biastoch et al., 2009, Barnier et al., 2020), the use of a local grid refinement in overflow regions is also investigated. The approach is to set-up a regional model configuration that includes an overflow region that is similar, in terms of resolution and physical or numerical parameters, to the global ocean eddying configurations widely used in the NEMO community. The DSO is chosen as test case because of its importance and the relatively large amount of observations available. Considering that mesoscale eddies are not fully resolved at this resolution, the focus is on the overflow mean product and not on the details of the dynamics as it is done in the very-high resolution (2 km) studies of Magaldi et al. (2015) and Koszalka et al. (2017).”

(Outlines of the paper)
“This work is presented in three parts. The first part (Section 2) presents the method used to carry out the sensitivity tests. It describes the regional NEMO z-coordinate configuration developed to simulate the DSO, and the initial and forcing conditions common to all sensitivity simulations. It also describes the simulation strategy and the diagnostics developed for the assessment of the model sensitivity. The control simulation that represents a standard solution is run and diagnosed. The second part (Section 3) describes the sensitivity of the modelled overflow to a large number of parameters. Results from about 50 simulations are used, spanning vertical resolution (46, 75, 150, and 300 vertical levels), horizontal resolution (1/12°, 1/36° and 1/60°), lateral boundary condition (free slip and no-slip), bottom boundary layer parameterization, closure scheme, momentum advection scheme, etc. The third part (Section 4) describes in details the DSO produced by our best solution. We conclude the study with a summary of the main findings and some perspectives to this work.”

We added the following references.

Almansi, M., T. W. N. Haine, R. S. Pickart, M. G. Magaldi, R. Gelderloos, and D. Mastropole, 2017: High-frequency variability in the circulation and hydrography of the Denmark Strait overflow from a high-resolution numerical model. J. Phys. Oceanogr., 47, 2999–3013, https://doi.org/10.1175/JPO-D-17-0129.1.

Barnier, B., Domina, A., Gulev, S., Molines, J.-M., Maitre, T., Penduff, T., Le Sommer, J., Brasseur, P., Brodeau, L., and P. Colombo, 2020: Modelling the impact of flow-driven turbine power plants on great wind-driven ocean currents and the assessment of their energy potential. Nat Energy ***5,*** *240–249. https://doi.org/10.1038/s41560-020-0580-2.*

Mathiot, P., Jourdain, N.C., Barnier, B., Gallée, H., Molines, J.-M., Le Sommer, J., and Penduff, T., 2012: Sensitivity of coastal polynyas and high-salinity shelf water production in the Ross Sea, Antarctica, to the atmospheric forcing. Ocean Dynamics 62, 701–723 (2012). https://doi.org/10.1007/s10236-012-0531-y.

Purkey S.G., Smethie W. M. Jr., Gebbie, G., Gordon, A. L., Sonnerup, R. E., Warner M. J., and Bullister, J. L., 2018: A Synoptic View of the Ventilation and Circulation of Antarctic Bottom Water from Chlorofluorocarbons and Natural Tracers. Annu. Rev. Mar. Sci., 10:8.1–8.25. https://doi.org/10.1146/annurev-marine-121916-063414.

Quadfasel, D., Käse, R., 2007. Present-day manifestation of the Nordic Seas overflows. In: Schmittner, A., Chiang, J.C.H., Hemmings, S.R. (Eds.), Ocean Circulation: Mechanisms and Impacts, Geophysical Monograph. American Geophysical Union, Washington. 10.1029/1 3GM07.

Spall, M.A., R.S. Pickart, P. Lin, W.v. Appen, D. Mastropole, H. Valdimarsson, T.W. Haine, and M. Almansi, 2019: Frontogenesis and Variability in Denmark Strait and Its Influence on Overflow Water. J. Phys. Oceanogr., 49, 1889–1904, https://doi.org/10.1175/JPO-D-19-0053.1

It would be great to have an illustration of spurious mixing due to advection+EVD.
In our “jargon”, “spurious” means “excessive and unphysical”. We make this clear in the texte (page 2 line 34).

"However, models using fixed geopotential levels as vertical coordinate (i.e. z-level models) are known to generate spurious (i.e. excessive and non-physical) diapycnal mixing when moving dense overflow waters downslope."

Quantifying the "spurious" mixing due to numerical schemes has been done in dedicated idealized simulation (e;g. Illicak et al., Ocean Modelling 45–46 (2012) 37–58), but we do not know how to do this in a realistic and forced model simulation. Therefore, we acknowledge that we are not able to provide such an illustration.

If other coordinates are better, why are z-coordinates used?
There is no single coordinate that fulfils all the needs of global OGCM (e.g. we do not know about a global implementation of a σ-coordinate model), all coordinates (e.g. geopotential, terrain following, isopycnal) having advantages and disadvantages. The final choice is always pragmatic. NEMO is an OGCM used by a wide scientific and operational community and it is certainly important, if not necessary, to document the sensitivity of the representation of key processes (like DSO) to model parameters.

No change in the text.

What observations and criteria have been used to identify "improvement"?
Except for the observations of Mastropole et al. (2017) displayed in Fig. 4 and ASOF6-section of Quadfasel (2004) displayed in Fig. 5, and the bottom temperature at moorings in Fig. 17, we do not use directly observations for our assessment. However, we do use published observations to assess qualitatively the results of our simulations. Qualitative comparison are made for Fig. 15 with the microstructure measurements from Paka et al. (2013), for Fig. 6,7 with the hydrographic sections from the ASOF project (Quadfasel, 2004) at sections 16, 20, 24 and 29.

The most used criteria to identify improvements between twins simulations is a colder bottom temperature of the DSO waters, as we explained page14, lines 1).
"From the large set of diagnostics performed to assess the impact of model changes on the DSO, it was found that the"analysis of the bottom temperature in the Irminger Basin is quite a pertinent way to provide a first assessment of the changes in the properties of the overflow. This diagnostic is consequently used to first compare the different sensitivity simulations, an additional diagnostics are used later for more quantitative assessments of the DSO representation."

Improvements are also identified if major flaws are reduced. These major flaws, identified on the time-mean properties of the overflow of the control simulation (section 2.3, 14-6 15-1,2), are: too warm bottom temperature, overflow depth not deep enough, weak temperature gradients between the plume and the ambient fluid (a not well-defined dense water plume).

We added a figure (Figure 5) comparing two experiments with observations at section 29 and provide more details on our assessment criteria in first paragraph of the Results section (Section 3, *Page 14 line 4):*
"Improvements between sensitivity tests are identified when one or several of the major flaws described in the previous section (section 2.3) are reduced. These flaws are; a too warm bottom temperature; an overflow not deep enough; and weak temperature gradients between the plume and the ambient fluid (a not well-defined dense water plume indicating too much dilution)."

*3. Please characterise the region: main parameters which are important for resolution of overflow: Rossby radius, Ekman depth and maximum/mean topography slopes, slope ratio for each resolution on the sill, as the authors have found this factor is most important. Ekman depth could be estimated from the bottom shear stresses: Hekm = Cdˆ0.5*U_bot/f (Thorpe, 1988) Soulsby (1983).*
This information is extensively described in the literature (see Quadfasel and Käse, 2007, for example). The first baroclinic radius of deformation is of the order of 20 km in the Irminger Sea. But this scale is not the one relevant to the instability of the dense water plume (a few kilometres, as we now mention in the introduction when mentioning the important processes).

Looking at the slope ratio for each resolution at and downstream the sill is difficult to use in a realistic setting since it varies greatly from a grid-point to another. This ratio is useful in the idealized experiment that we discuss in Fig. 10 and is chosen to be 5.

The comment on the Ekman depth led us to add a comment regarding its resolution with the vertical resolutions used. This is done in the appendix A in the discussion of Fig. A1 which compares the various vertical resolutions used in the study.

Text added in Appendix A (page 29, line 15):
"***Vertical Resolutions used:*** *The variations of the cell thickness as a function of depth is presented in Fig. A1 for the four different vertical resolutions used. A rough estimate of the bottom Ekman layer is given by* $h_E = \kappa U_*/f$ *(Cushman-Roisin and Beckers, 2011) yields* h_E *= ~45 m in our present model setting for an overflow speed of 0.5 m/s and* U_* *being calculated from the quadratic bottom friction of the model. Consequently, in the 600 m to 1500 m depth range that correspond to the initial depth range of the overflow, the bottom Ekman layer will only be partially resolved for model vertical resolution of ~10 to 15 m near the bottom, which according to Fig. A1 will happens only for a model resolution of 150 levels (2 to 3 points) and 300 levels (5 to 6 points)."*

We refer to this appendix in the description of the model configuration (Section 2.2, page 6 line 1):
"The cell-thickness as a function of depth is shown in Appendix A (Fig. A1) and the resolution of the bottom Ekman layer in the different vertical resolution settings is discussed."

Reference added:

Cushman Roisin B. and Beckers J. M., 2011: Introduction to Geophysical Fluid Dynamics , Physical and Numerical Aspects. Academic Press, Chap. 8, 219-246.

4. Winton 1998 experiment: "To show the effect of this concept, we simulate the descent of a continuous source of cold water down a shelf break in an idealized configuration of NEMO (with no rotation, comparable to that of Winton et al. (1998))." It is not the Winton, 1998 experiment. Winton compared with an EKMAN – type solution, so the dynamics was rotationally important, his solution was 2D on the f-plane. The solution, shown in fig 9 (Fig. 10 in revised version) is not relevant to the baseline study. You consider (fig 9) the propagation of dense boundary layer in a barotopic fluid with a very weak density difference in the plume and ambient waters (0.5C over 3000m depth). So, the balance is between gravity force and friction.

We agree that we do not reproduce the experiment of Winton et al. (W1988). We only illustrate the concept exposed by the schematic shown in the Fig. 7 of W1988 which does not imply rotation. We realize that our inappropriate reference to the paper of Winton et al. (1988) is the cause of a misunderstanding regarding the purpose of the idealized simulation used to produce our Fig. 10. Our idealized simulation only aims at illustrating how the hydrostatic model NEMO propagates dense water downward a slope, and how this process depends on the vertical resolution. This process is described in Section 2.1, page 6, lines 13-18.
In the idealized set-up of Fig. 10, the dynamics are dominated by advection (driven by horizontal pressure gradient) and diffusion. The model is hydrostatic, so there is no gravity force. Vertical motions are driven by vertical diffusion, and divergence of the horizontal flow that sets the vertical velocity (through non-divergence). Finally, we point out that the ambient fluid is not barotropic but homogeneous, and the density difference between the plume and the ambient fluid (5°C, not 0.5°C) is not weak.

The fact that the realistic model follows this paradigm is illustrated in Fig. R3.4 for the 1/60° resolution and Fig. R3.5 for the 1/12°, attached to our response to the review. It shows (at section 12 from the sill) that the front of the plume, defined by the 28.85 isopycnal is progressively sinking to great depth under the effect of a negative Richardson number (i.e. under the effect of the EVD parameterization).

The text is modified as follows, removing reference to W1988 where we think not appropriate and bring confusion:

Page 16 line 27:
"An explanation to this is searched for following the paradigm exposed in Fig. 7 of Winton et al. (1998) which states that the horizontal and vertical resolutions should not be chosen independently: the slope of the grid ($\Delta z/\Delta x$) has to equal the slope of the topography (α) to produce a proper descent of the dense fluid."

Page 16 line 32:
"To show how NEMO follows this concept, we simulate the descent of a continuous source of cold water down a shelf break in an idealized configuration (with no rotation)." ~~*comparable to that of Winton et al. (1998)).*~~

Page 18, lines 1-4:
"In that regime, the overflow simulated in the 300 vertical levels run (i.e. with 5 a local grid slope smaller than the topographic slope) presents warmer bottom waters (Fig. 9a) than in the 60 levels run, ~~*validating to a certain extent the rationale exposed in Winton et al. (1998)*~~ *and in agreement with the results obtained with the realistic DSO12 configuration."*

Also, you cannot claim that the second case (9b) is worse or better! Is this an effect of EVD or as twice as strong shear, seen in the panel 9b? It is not clear, that solution 9a are physically more consistent compared with 9b.
We agree. In both simulations, the plume propagates downward, essentially due to the high values of the vertical diffusivity (EVD) resulting from the static instability (due to advection of dense fluid over lighter fluid). The bottom water of the plume is colder in the 50 m resolution (60 levels) than in the 10 m resolution (300 levels). Therefore, we consider that the low-resolution case is better regarding the downslope propagation of the cold bottom temperature. We also consider that the upper part of the plume is more coherent in the 10 m resolution case due to a better resolution of the vertical shear (the *tke* scheme being sensitive to vertical resolution). This is explained in pages 17 and 18 in the paper (we removed the reference to Winton 1988 in this part as our idealized simulations do not address the same problem), a paragraph that we reproduce below emphasizing in magenta color the sentences that address these two points:

"In the absence of rotation, the pressure force pushes the blob over the shelf break and the EVD mixing scheme propagates the cold water down to the bottom as the blob moves toward deeper waters, generating an overflow plume. After about 5 days, the front of the plume has reached the end of the shelf break and entered the damping zone at the right side of the domain, reaching a quasi-stationary regime. In that regime, the overflow simulated in the 300 vertical levels run (i.e. with a local grid slope smaller than the topographic slope) presents warmer bottom waters (Fig. 10a) than in the 60 levels run in agreement with the results obtained with the realistic DSO12 configuration. Note that the vertical shear is more confined in the high-resolution case, which prevents the upward extent of the TKE induced mixing of the upper part of the overflow that is seen in the low-resolution case. Thus, the plume is more consistent in the high-resolution case but present warmer bottom waters. Note that when using a realistic bottom topography, the topographic slope will present large local variations and that it will be almost impossible to match the two slopes over the whole domain in a z-coordinate context. Therefore, increasing the number of vertical levels will not systematically degrade the overflow representation everywhere."

If you want comparisons with analytical solutions, I recommend reproducing Shapiro & Hill 1997 analytical solutions for cascading. This is not completely overflows (entrainment is weak), but it is a good test, as approved also by laboratory experiments, (Wobus et al, 2009 and Bruciaferri et al, 2018).
We retain the suggestions for future work testing new parameterization of non-hydrostatic effects.

My recommendation is to remove this paragraph from the paper, as it is not relevant to the study.
Having clarified the purpose and context of the idealized simulation and removed the inappropriate link to W1998, we retain this part because we consider it is a good illustration of our interpretation of the behaviour of the cascading in the realistic configuration.

5. I am not convinced that using EVD is a single source of increased simulated mixing when increasing the number of vertical levels. The authors state: What other processes that model start to resolve at finer vertical resolution could affect generation of strong shear and mixing, as inertial or internal waves, topographically

trapped Rossby waves? Please, look at high frequency variability at the water column, say, using a Hovmöller diagram. Fig 13a,c, shows the presence of small-scale (and probably high frequency) features. To my mind it shows presence of internal waves of high amplitude.

We do not pretend that EVD is the single cause of increased simulated mixing, and the properties of the overflow waters are certainly influenced by other mixing processes (*TKE* or numerically induced) than EVD. The *TKE* closure scheme is NEMO, like many other similar schemes, is consistent with an instability criterion based on a Richardson number (*Ri*). For this reason, the reviewer is right (in the next comment) when suggesting to look at *Ri*. For weak stratifications and significant shear, *TKE* provides large values of *Kz*, sometimes as large as the 10 m^2s^{-1} used in EVD. EVD is just a way to "boost" the TKE values in case of static instability ($N^2 > 0$).

In NEMO, the downslope cascading of dense waters from a bottom cell to a deeper bottom cell, which would be driven by vertical acceleration in a non-hydrostatic model, is made by the EVD vertical mixing. Therefore, the dense waters do not sink and accelerate downward but are mixed. Other processes have an impact on the simulated mixing, but by construction of the model, they are not dominant in the representation of the cascading.

The attribution of the high values of the vertical diffusivity coefficient (*Kz*) shown above the 27.85 in Fig.13a,c (1/60°) and not seen in Fig.13b,d (1/12°) is clearly a removal of static instability by EVD, as demonstrated in Figure R3.1 below, which shows hourly value of *Kz* and *Ri* at section 20 at two different times separated by 17 hours. The large *Kz* values between isopycnal 27.80 and 27.85 at hour 254 (Fig. R3.1a) are associated to negative *Ri*, indication removal of a static instability, thus mixing by EVD. At hour 271 (17 hours later, Fig R3.1b), the stratification is stable and *Kz* does not present anymore large values between those isopycnals.

We analysed this period in details (see Fig. R3.2 and Fig. 3.3 attached to this response), and we found that it correspond to the passage through the section of a bottom intensified cyclonic eddy (a bolus of overflow water). The core of the cyclonic eddy (Fig R3.2a), the tangential flow is off-shore and pushes dense water over lighted water, which generate static instability and turns on EVD. The dense water mixes with lighter water below. In the tail of the cyclonic eddy (Fig. R3.2b), the tangential flow is on-shore and does not generate static instability. This does not happens at 1/12° because the horizontal resolution is not enough to well resolve the boluses.

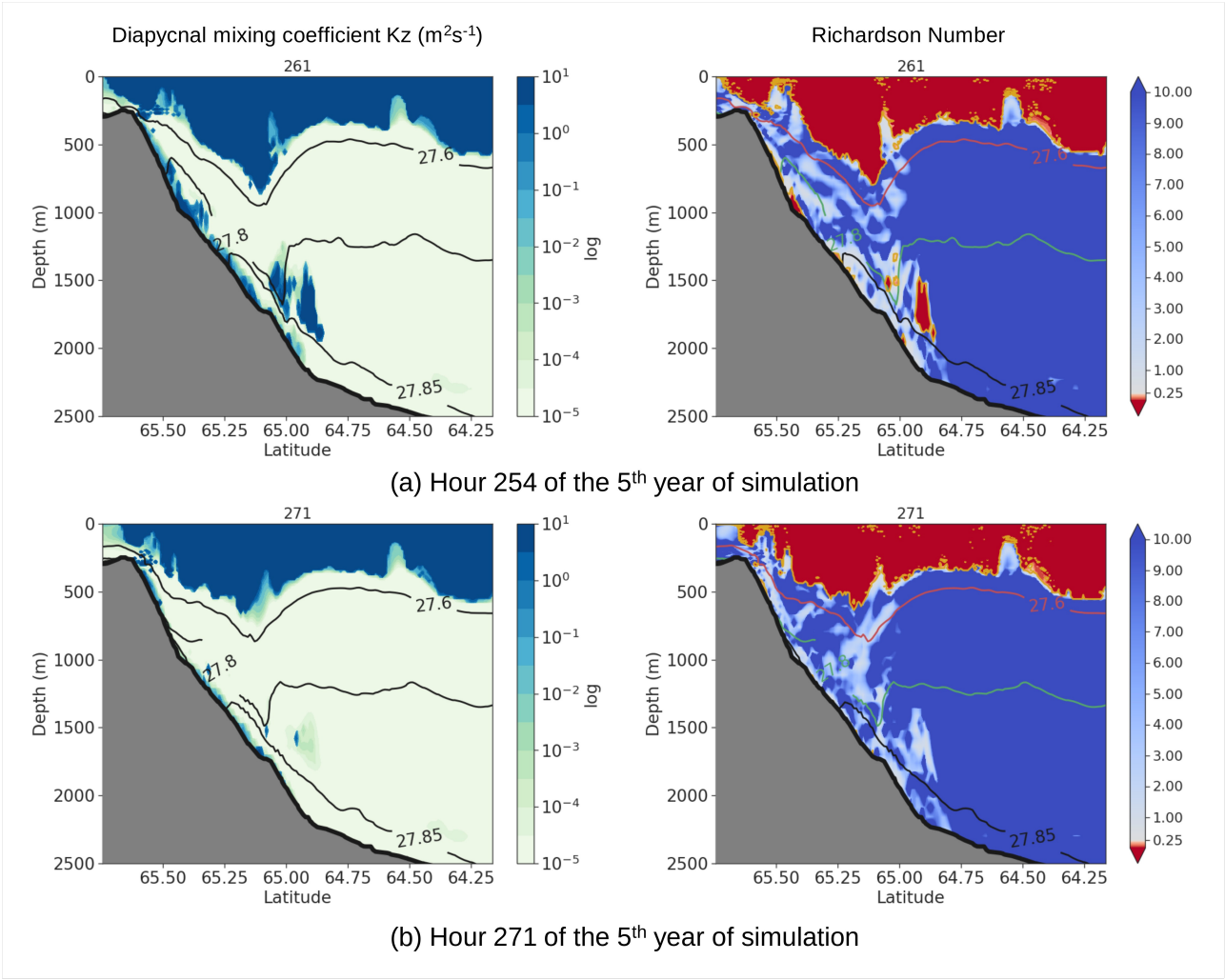

(a) Hour 254 of the 5th year of simulation

(b) Hour 271 of the 5th year of simulation

Figure R3.1: Hourly values of the vertical mixing coefficient Kz and of the Richardson number Ri across section 20 at two different times. Ri values of 0.25 are contoured in yellow. Negative Ri values are in dark red.

Therefore, our interpretation that this intermittent, but intense mixing event between those isopycnal is driven by EVD is correct.

Changes in the revised paper:
We modified Fig. 14a,c by picking two different times (those in the Figure above) when this mixing is present and when it is not, to illustrate its intermittency.
We do mention, without providing detailed explanations, that this feature is not seen in the 1/12° it is because it is driven by the cyclonic boluses not resolved at that resolution (section, page 21 line 16):
"In the case of DSO60.L150 (Fig. 14a,c) a small but noticeable mixing remains confined to a very thin bottom layer below the 27.85 isopycnal, and very little mixing occurs in the core of the overflow plume. Intermittent static instabilities occur between the 27.85 and the 27.8 isopycnals (shown by the large values of Kz in Fig. 14a). Our analysis (no figure shown) indicates that these instabilities are generated by advection toward the deep ocean of bolus of dense water by a cyclonic bottom intensified eddy. After the eddy passed through the section (Fig. 14c) the stratification is again stable. Such feature are not seen in the 1/12° simulation (Fig. 14b,d) because the horizontal resolution does not resolve properly the mesoscale eddies."

6. Another possible cause of an enhanced mixing in the fine vertical resolution is a parameterisation of diffusivity set in a weakly stratified condition. Indeed, in TKE vertical mixing scheme (and gls scheme in an strongly stratified conditions), the turbulent length scale is set as l= 0.1* TKEˆ(1/2)/N and vertical diffusivity AVT∼TKE/N, where TKE is a turbulent kinetic energy, defined by the tke equation but larger by some background value, N is a buoyancy frequency, which differs due to resolution. Subcritical Richardson numbers (Ri<Ricr∼1/4), responsible for generation of small –scale turbulent mixing are also vertical

resolution dependant. Let us consider a plume of dense water of constant density ro_plume propagating downslope in unstratified fluid (of density ro_0) with velocity U. Velocity shear is S=U/dz, the Richardson number at the edge of the plume is

Ri=N^2/S^2=g(Ro_plume –Ro_0)*dz/(U^2*roo)

will be smaller at the finer vertical resolution which results in more mixing entrainment on the top of the dense plume. This could be examined by comparison of statistics of occurrence the negative (EVD effects) and small positive Richardson numbers at the edge of plume simulations with different resolutions. The other possibility is to check this assumption, to evaluate the number of occurrence of AVT exactly fit to EVD parameterisations (10m^2/s, convection) and in the smaller range (~0.001-1m^2/s, Kelvin-Helmholtz instability). In the 1/12 resolution, (Fig 8, Fig 9 in the revised paper) I see combination of open-ocean convection (EVD) and shear instability turbulence. How do you explain a much larger area of open convection in the figure 8b, identified by 5-year mean very strong mixing from the surface to the bottom? May be at some point the water of other origin penetrates from the surface to the bottom and mixes with propagating plume?

We acknowledge that we did not count the occurrences of EVD. This must be done on-line during integration and this was not in the I/O part of the code, so we stored hourly mean values (i.e. averaged over 8 time steps) to have an estimate of the high frequency motions. One single EDV event will produce a $Kz > 1$.

We calculated the Richardson number *Ri* as suggested by the reviewer. As shown in Fig. R3.1 above, *Ri* and *Kz* are very consistent, which demonstrate that the *TKE* closure behaviour is very consistent with the stability criterion based on the Richardson number (which is expected). Note that since *Ri* and *Kz* provide almost the same information we do not show *Ri* in the paper.

We modified Fig. 9 and show the mean summer situation, so the winter mixed layer is not present, which allows to better focus on intermediate depths (see below).
It shows that the large *Kz* values between isopycnals 27.6 and 27.8 are not driven from the surface but are generated locally at mid depth. They are driven by the vertical shear existing between the northward surface current passing through the Denmark Strait (the NIIC) which is very variable in position and intensity, and the southward deep current carrying the overflow waters. We notice that the mixing is greater in the high resolution case. Several studies (e.g. Spall et al 2019) show that the NICC can occupy for short periods (few hours to day) the whole strait blocking the passage of the overflow. Our study does not focuses on this process although it is reproduced in our simulations, but of the descent of the dense waters. So our analysis first focuses on the *Kz* near the bottom (below isopycnal 27.85 or 27.8) and then we discuss the values of *Kz* at intermediate depths (Page 16 Line 19):
"The vertical diffusivity along the path of the overflow is shown in Fig. 9 for the 46 and the 300 level cases (the definition and method of calculation of the overflow path are given in Appendix B). Compared to the 46 level case, the 300 level case (Fig. 9b) exhibits greater values of the diffusion coefficient near and above the bottom along the path of the overflow. This enhanced mixing affects the overflow plume, which 200 km after the sill does not contains waters denser than 27.85, while such waters are still found 300 km down the sill in the 46 level case. The 300 level case also exhibits large values of diffusion coefficient at intermediate depth (between isopycnal 27.8 and 27.6). They are driven by the vertical shear existing between the northward surface current passing through the Denmark Strait (the NIIC) which is very variable in position and intensity, and the southward deep current carrying the overflow waters (e.g. Spall et al 2019). We notice that the mixing is significantly greater in the high resolution case, which indicate that this process could also contribute to the dilution of the overflow plume. However, it does not seem to affect the thickness of the 27.8 isopycnal."

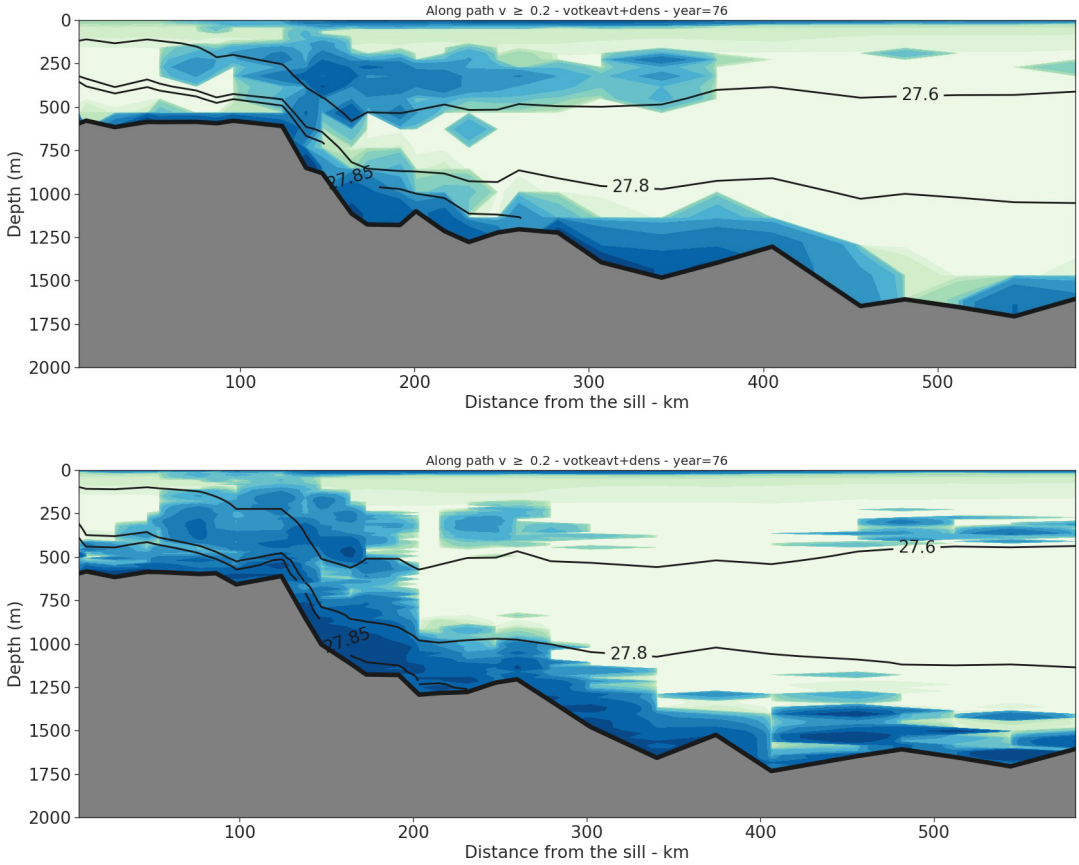

"Figure 9. Summer mean (5th year of simulation) of the vertical diffusivity coefficient along the path of the vein calculated for a) simulation DSO12.L46 and b) simulation DSO12.L300. Potential density values (_0) are shown by the contour lines colored in red (27.6), green (27.8) and black (27.85)."

7. Check consistency of bottom topography, specifically in the "worst case" L300. The authors state: "Bottom topography and coastlines are exactly those of the global 1/12 ORCA12 configuration and are not changed in sensitivity experiments, except when grid refinement is used. In this latter case the refined topography is a bi-linear interpolation of that at 1/12, so the topographic slopes remain unchanged". It is not seen from the figure 8, where bottom topography is different in simulations L46 and L300. Does adjective TVD scheme work similar in the different vertical resolutions?
Topographies are different because the path of the overflow in DSO12.L46 is different from the path in DSO12.L300 (Figure in appendix B).
The model uses a partial step bottom topography, which means that the thickness of the bottom level is adjusted to the real bottom depth. Therefore, the depth does not change when the vertical resolution changes, as it may be the case when a full cell representation of the bathymetry is used (is that latter case the bathymetry is changed to adapt to the thickness of the bottom cell). When horizontal resolution is increased, the topography is linearly interpolated, so the slope is not changed. The consistency of the topography of all simulations can be checked by looking at the bathymetric contours in figures 8, 11 and 12: they are all identical.

Minor comments:
Abstract: What observations and criteria have been used to identify "improvement"?
This is now better explained in the paper and does not need to be explicit in the abstract.

Contrary to expectations, in the given numerical set-up, the increase of the vertical resolution "It is found that when the local slope of the grid is weaker than the slope of the topography the result is a more diluted vein. Such a grid enhances the dilution of the plume in the ambient fluid and produces its thickening. Although the greater number of levels allows for a better resolution of the ageostrophic Ekman flow in the bottom layer, the final result also depends on how the local grid slope matches the topography" It is known

result from Winton et al. (1998), that the model should resolve slopes and Ekman layer, so if slopes are not resolved, vertical resolution cannot help.
We removed "contrary to expectation" as this could have been expected, although surprising that this still holds at 1/60° and 300 levels. This could be specific to the NEMO code.

1. From introduction it is not clear, what is overflow, how it is formed and what processes dominates in the dynamics. Even for pure numerical –oriented paper it is important to understand, what should be in the equations and why this resolution is chosen. "An oceanic overflow is a dense water mass" – is this a water mass (object) or process?
We accounted for these comments when revising the introduction of the paper to respond to the second major comments of the reviewer.

"Overflows of important magnitude are" – what do you mean under important magnitude?
We agree that the use of magnitude was not appropriate. We cite the overflow that are important for the general circulation. The text is now:
"Overflows of importance because of their contribution to the general circulation are …"

"is balanced by the intrusion of waters from regions different from where the overflow waters are formed" – please, rephrase it. "For example, the flux of cold waters formed in the Arctic Ocean and the Nordic Seas that enters the North Atlantic with the Denmark Strait and Faroe Bank Channel overflows is balanced by warm and salty Atlantic waters that flows over the Iceland-Scotland Ridge towards the Arctic Ocean via upper ocean currents" It sounds as Atlantic Warm currents are caused by compensation to overflow.
Many model studies have demonstrated that in the Atlantic Ocean, weak overflows result in a weak AMOC (e.g. Willebrand, 2001) which is turn reduced the meridional heat transport associated with the northward flowing warm Atlantic waters. In order to simplify the introduction already rich of information we just mention the contribution of the DSO to the deep circulation of the North Atlantic:
"For the case of the Denmark Strait overflow (DSO hereafter), it feeds the Deep Western Boundary Current in the North Atlantic, and so contributes to the Atlantic Meridional Overturning Cell and the global thermohaline circulation (Dickson and Brown, 1994, …"

"However, the dynamical processes that control overflows have rather small scales" – please, emphasise what small scales processes. What is the main balance in the overflows? Why spurious mixing is considered to be strong? It is not clear from the introduction. Refer to the paper, or just point out what is wrong due to spurious mixing (volume flux, salinity , temperature?)
We consider that the important changes made to the introduction respond to this comment, as processes, scales of motions are addressed, and spurious mixing is defined…

5. You mention the importance of non-hydrostatic physics and then mention Magaldi & Haine, 2015 paper (correct reference) showing different contrary results (see also Wobus et al, 2011).
"They also characterized the dependence on various model parameters regarding the mixing of the overflow waters with ambient waters." – I don't understand what do you mean here: mixing depends on parameters? Or something else, which parameters?
Our comments regarding the dependence on various model parameters concern the studies of Magaldi et al., 2011, … , which use the hydrostatic version of the MIR GCM, and in this version, the diapycnal mixing is "parameterized" by a turbulent closure scheme since there is not vertical acceleration (the vertical momentum equation being reduced to the hydrostatic pressure equation). These schemes have parameters to be tuned.
"Most recent high-resolution regional modelling studies of the Denmark Strait overflow (Magaldi et al., 2011, ~~2015,~~ Koszalka et al., 2013, 2017, Almnsi et al., 2017, Spall et al., 2019) or the Faroe Bank Chanel overflow (Riemenschneider and Legg, 2007, Seim et al., 2010) have been using hydrostatic model configurations of the MIT OGCM."
We remove the reference to Magaldi and Haine (2005) in this sentence, although relevant but confusing since this study is cited just above for the use of hydrostatic models.

"found a greater sensitivity of the mixing to horizontal resolution and, but to a lesser extent, to vertical resolution and vertical viscosity" is it resolved horizontal or vertical mixing? Or spurious? How mixing have been examined?

We modified this to emphasize only the sensitivity of resolution, most relevant for our study:
"For the case of the Faroe Bank Channel overflow for example, Riemenschneider and Legg (2007) found the greatest sensitivity of the mixing in changes in horizontal resolution. ~~The sensitivity to other parameters tested (bottom drag coefficient, strength of the inflow) were found to be minor.~~"

"but not the small-scale diapycnal mixing which still needs to be fully parameterized by the turbulent closure scheme." – please, rephrase it. It is true of course, as to resolve diapycnal mixing you need scales up to the dissipative one, which is of 1mm.
We rephrased it as we modified the introduction.
"Diapycnal mixing processes (e.g. entrainment of ambient waters into the cascading plume by shear-driven mixing, bottom friction, internal wave breaking) have even smaller scales (a few meters to a 1 mm) and cannot be resolved in present ocean models. Their effects are represented by a vertical turbulence closure scheme, the aim of which is to achieve a physically-based representation of this small-scale turbulence."

" a resisting bias in this type of model simulations are likely to contribute." – what is resisting bias?
A resisting bias is a bias that is not sensitive to the model parameters and cannot be corrected by parameter optimisation. Correcting the bias will require the development of new parameterisations. In the present case, it is more correct to use the word "persisting bias".

We now use "persisting bias" as bias that we haven't corrected.

Page 11: "The detailed list of theses experiments"
Corrected

Page 19: (15)
"In the case of DSO60.L150 (Fig. 13a,13c) the EVD driven mixing remains confined to a very thin bottom layer below the 15 27.85 isopycnal and very little mixing occurs in the core of the overflow plume" - If you look at the magnitude of near bottom mixing, it is too small to be EVD, probably is it shear-driven Ekman layer;
Yes. As we show in Fig. R3.3 added to this review, the EVD mixing is usually acting at the head of the plume and not inside. So within the plume, the mixing is due to the local shear (TKE), but it can be very large in the from of the plume during the phases when it is sinking.
In the paper, we use, to be consistent with the figure:
"… small but noticeable mixing …"

" Intermittent static instabilities occur between the 27.85 and the 27.8 isopycnals, the associated mixing being small since the temperature and salinity gradients are quite small there" - Figure shows very strong mixing>1mˆ2/s of high frequency and small scale. As T,S differences are small, Ri numbers to be small there, resulting in a strong intermittent mixing. What frequency and scales are? Is it small positive Ri (Kelvin-Helmholtz instability), or negative Ri (convection, EVD)?
We clarified this when discussing Fig. 14a,c.

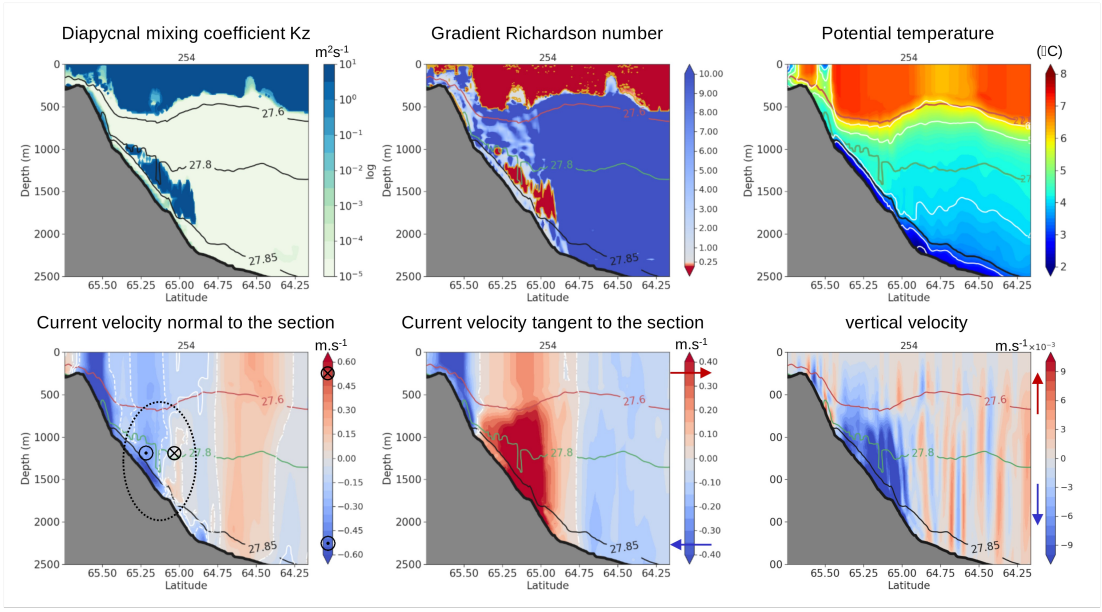

(a) Hour 254 of year 5

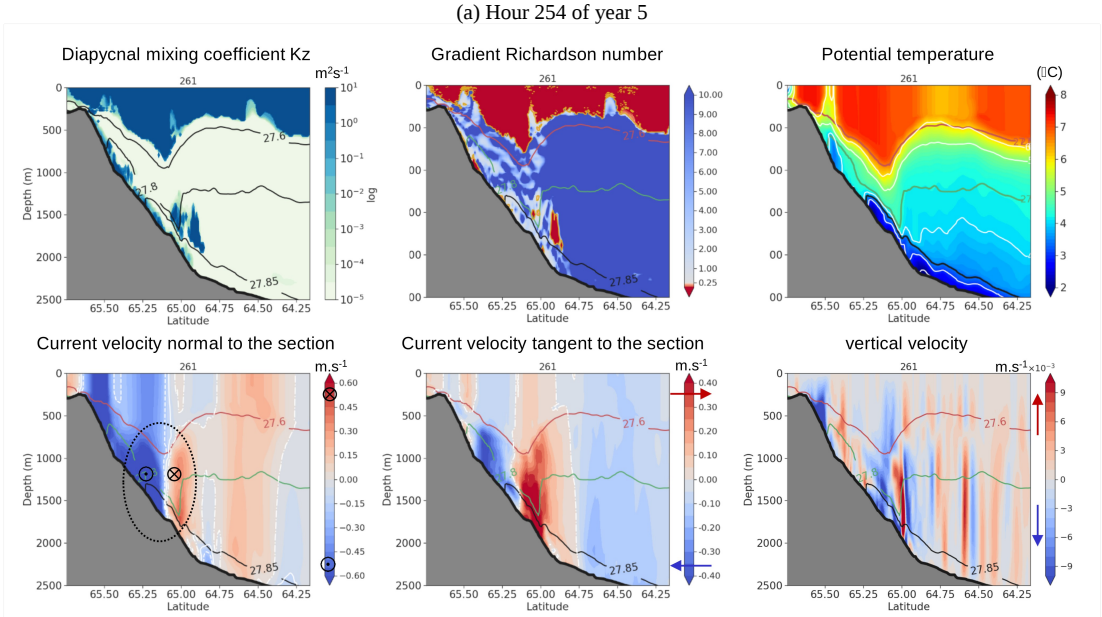

(b) Hour 261 of year 5

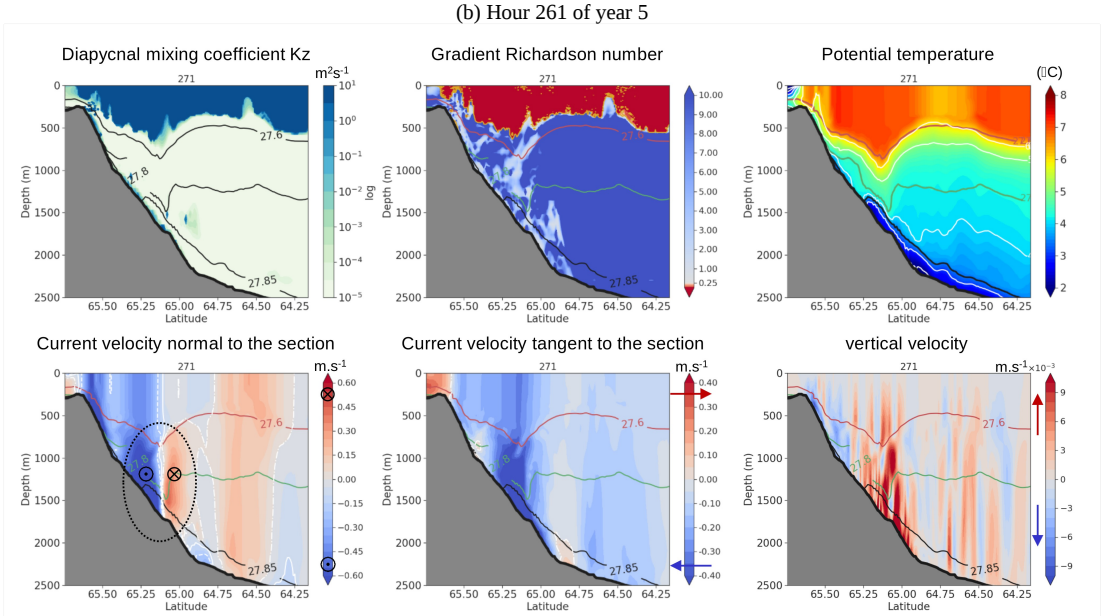

(c) Hour 271 of year 5

Fig. R3.2: Characteristics of the instantaneous (hourly mean) circulation at Section 12 after the sill in simulation DSO60.L150 (1/60°, 150 levels) at three different times. (a) Situation at hour 254 before the arrival of cyclonic eddy. (b) Situation at hour 261 when the bottom intensified cyclonic eddy is passing through the section. (c) Situation at hour 271 when the tail of the eddy is captured (see also Fig. R3.3). The cyclonic eddy is outlined by the dotted line circle in the panel showing the velocity normal to the section

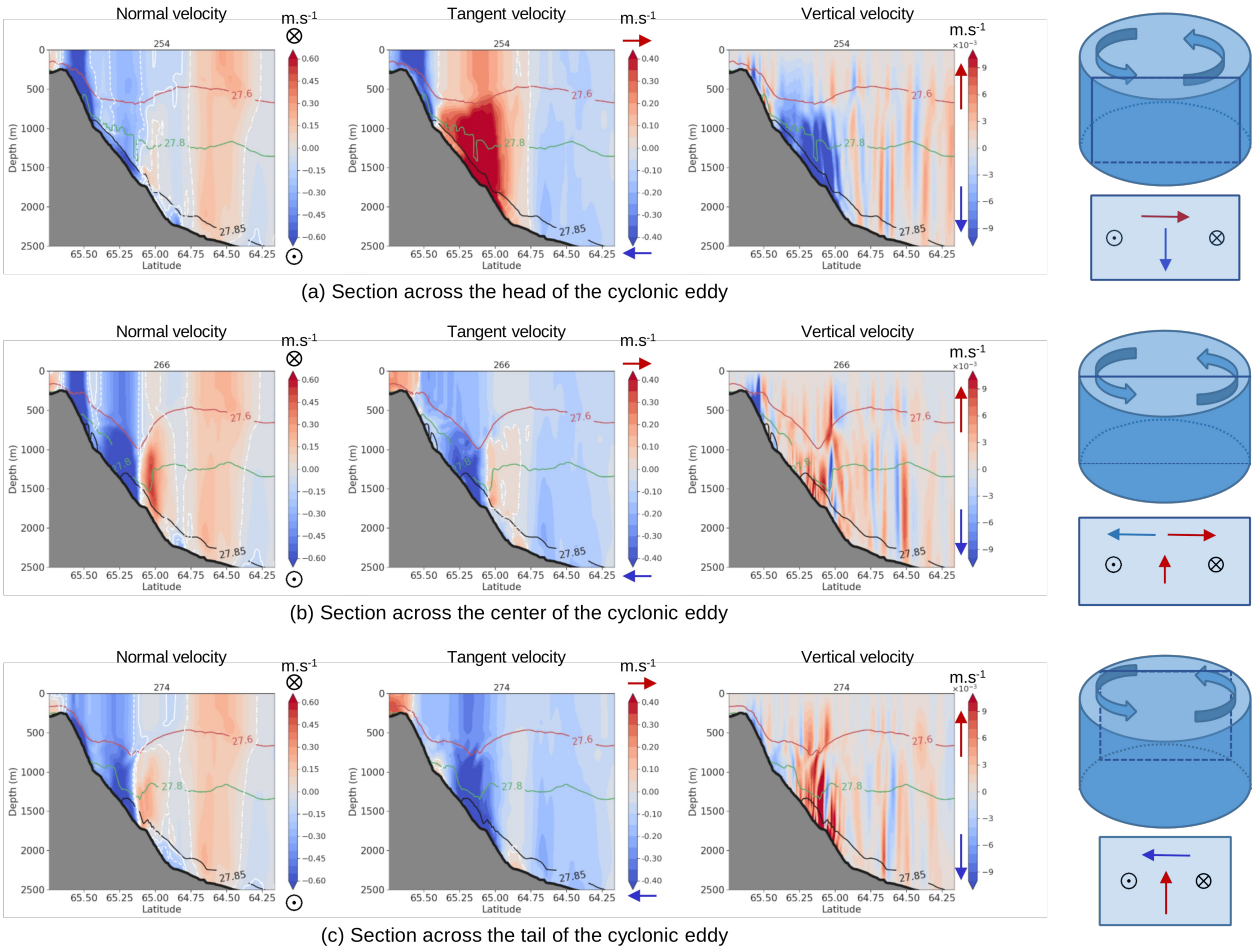

(a) Section across the head of the cyclonic eddy

(b) Section across the center of the cyclonic eddy

(c) Section across the tail of the cyclonic eddy

Fig. R3.3: Simulation DS060.L150. Components of the current velocity at Section 20 Schematic illustrating the passage of a cyclonic eddy. Schematics on the right summarise the organisation of the velocity field.

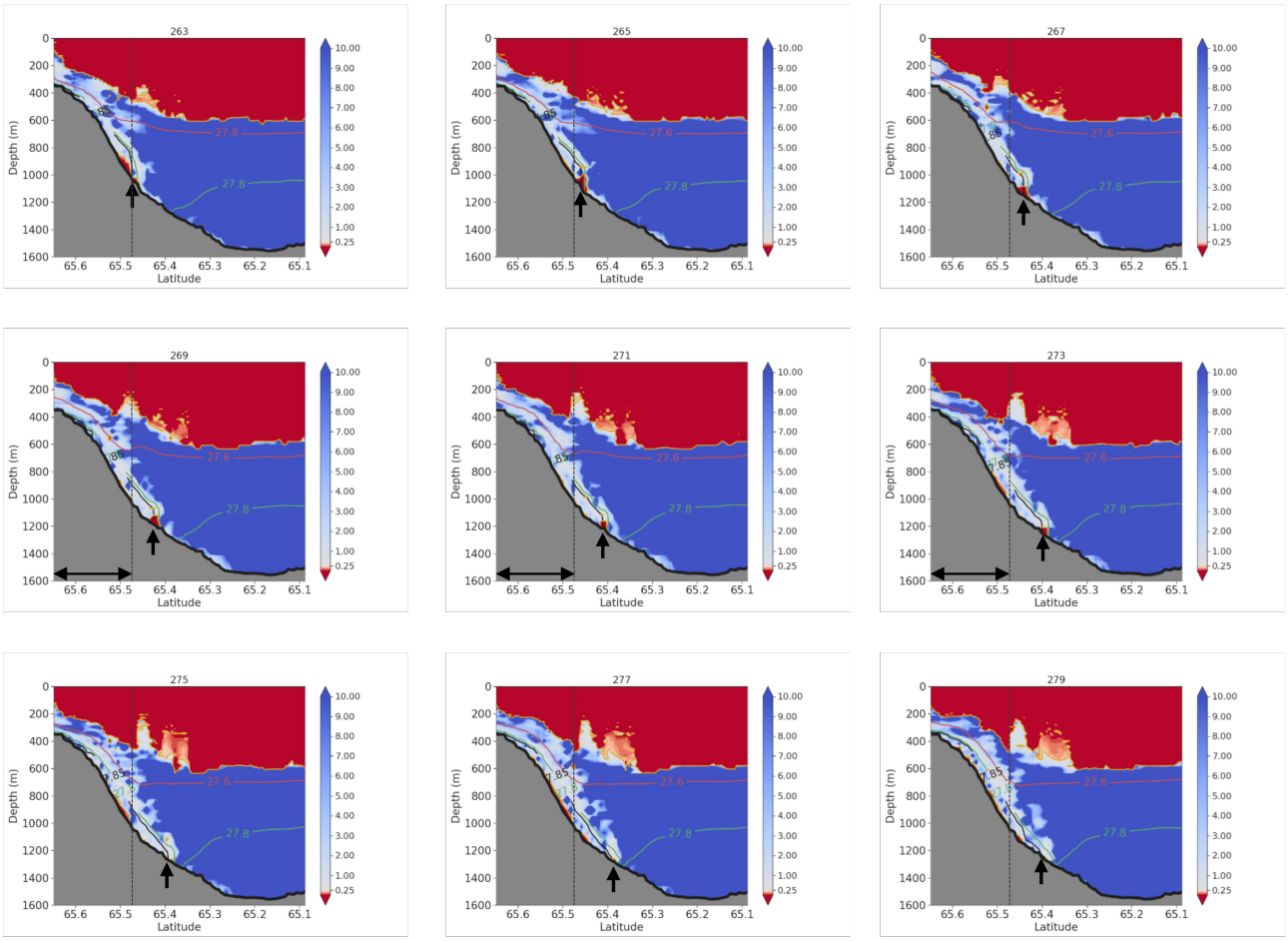

Fig. R3.4: Simulation DSO60.L150. Evolution of the hourly Richardson number, *Ri*, at section 12 over a 18 hours period (a plot every 2 hours). Negative values and values below 0.25 are colored in Red. The 0.25 contour is shown in yellow. Isopycnals 27.6, 27.8 and 27.85 are plotted in red, green and black respectively. The black arrows show the position of the front of the overflow plume defined as the deepest location of the 27.85 isopycnal, and the vertical dotted grey line indicate the initial position of the front at hour 263. As the front deepens with time, it is always associated with negative values of *Ri* which indicate that the EVD is turned on, illustrating the sinking of dense waters by the EVD parameterisation.

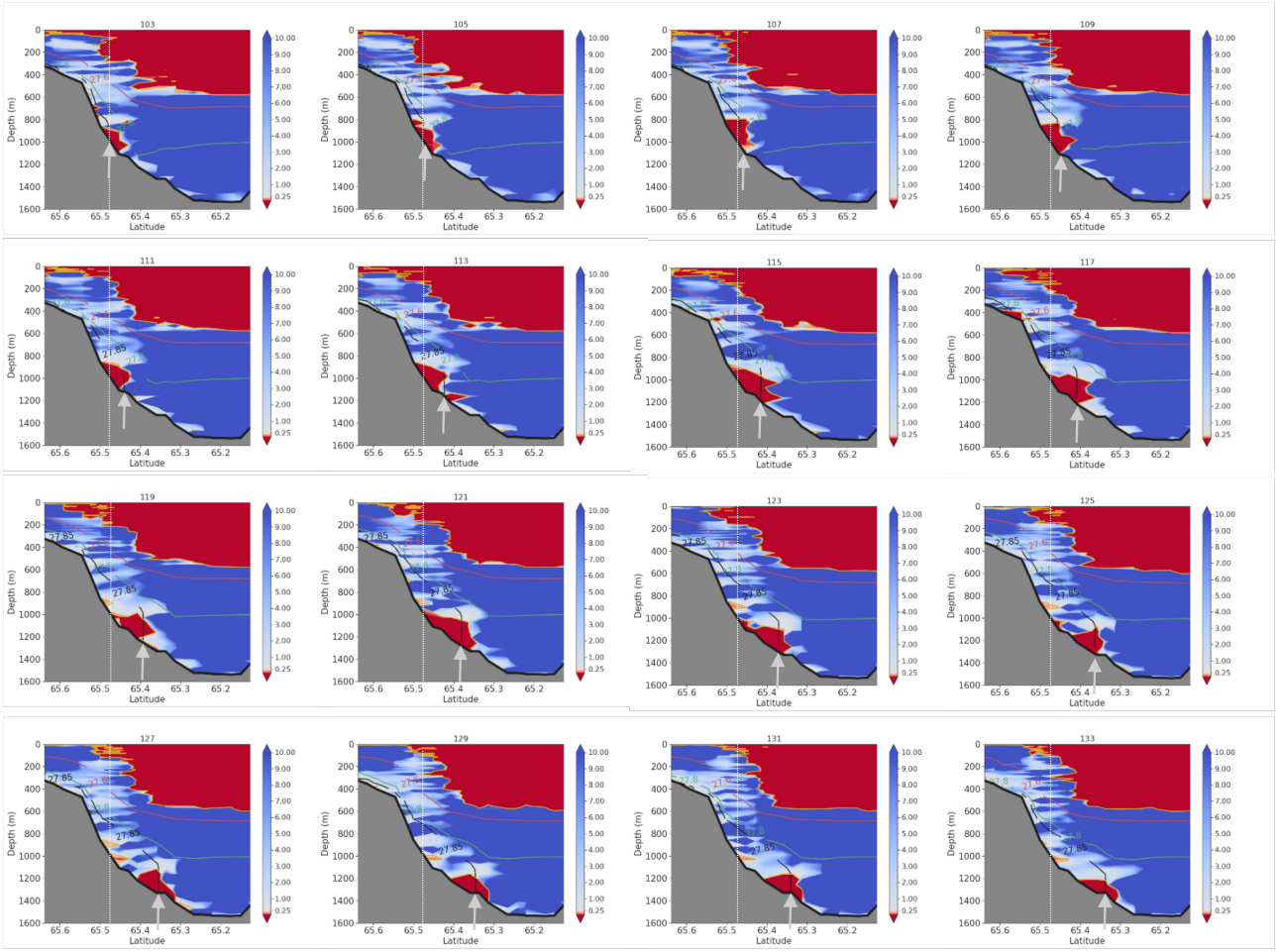

Fig. R3.5: Simulation DSO12.L150. Evolution of the hourly Richardson number, *Ri*, at Section 12 over a 32 hours period (a plot every 2 hours). Negative values and values below 0.25 are colored in Red. The 0.25 contour is shown in yellow. Isopycnals 27.6, 27.8 and 27.85 are plotted in red, green and black respectively. The grey arrow show the position of the front of the overflow plume defined as the deepest location of the 27.85 isopycnal, and the vertical dotted grey line indicate the initial position of the front at hour 103. As the front deepens with time, it is always associated with negative values of *Ri* which indicate that the EVD is turned on, illustrating the sinking of dense waters by the EVD parameterisation.